放送大学研究年報　第19号（2001）113-143頁
Journal of the University of the Air, No.19 (2001) pp.113-143



# Vibrational Circular Dichroism Spectroscopy
## －A method of studying chiral molecules－

Yoshiaki HAMADA[*1)]・Saeko SHIN[*2)]

# 振動円偏光二色性分光法
## －キラル分子を調べる方法－

濱　田　嘉　昭・新　佐依子

## 要　約

分子のキラリティーは生命の基本的な役割を担っている。アミノ酸や糖には二つの立体化学的な異性体が存在する。すなわち、左手と右手の関係の構造である。これらの光学活性の性質をそれぞれ、円偏光二色性および施光性という。円偏光二色性の理論的基礎についてまとめた。これらは古典的な電磁気学と現代の量子力学によって基礎づけがなされており、電気双極子遷移モーメントと磁気双極子遷移モーメントの内積がゼロでない値を持つことが、光学活性の発現に必要であることを示している。両理論の結果を比較し、導出された式の関係づけを行った。

本論文の最後には、著者らが行った振動円偏光二色性実験の予備的な結果を述べた。環状分子を用いて、純理論計算による実測スペクトルの予測と解釈の性能を検討した。また、アミノアルコールを用いた実験では、多数の立体配座の存在と水素結合がある分子系の溶液構造を研究する際に、振動円偏光二色性を用いることの潜在的可能性を検討した。

## ABSTRACT

Molecular chirality plays a fundamental role in life. The amino acids and sugar have two stereochemical isomers. That is, there are left-handed and right-handed forms. They show the different features to circularly polarized light. The efficiency of absorption is different and rotates the polarization axis. These optical activities are called circular dichroism and optical rotation, respectively. Theoretical bases of circular dichroism are reviewed. They are derived by classical electromagnetism and also by quantum mechanics, and indicate there needs a nonzero value of the inner product of electric dipole transition moment and magnetic dipole transition moment to gain the optical activity. The formulae from the classical and modern theories are compared and correlated.

At the last part of this review article, we report our preliminary results of

*1) 放送大学助教授（自然の理解）
*2) 放送大学教務補佐員（自然の理解）

vibrational circular dichroism measurement of a ring compound to investigate the ability for prediction and analysis of the observed spectrum by using purely theoretical calculation. We also report the potential ability of vibrational circular dichroism for studying the molecular structure in solution, particularly the complicated system where there is a conformational multiplicity and hydrogen bonding.

There is a stereoisomerism, called enantiomerism, in α-amino acids as the components of protein and polypeptide, and in 2-deoxyriboses that make skeletal units of DNA. Each enantiomer makes the linearly polarized light rotate its axis of the polarization after the light passes the sample. This optical activity arises from the existence of the two mirror-imaged forms in the amino acids and riboses. The term, chirality, is also used for the characteristic that the real image and mirror image cannot be overlapped exactly. The α-amino acids and 2-deoxyriboses in all lives on the earth have L- and D-forms, respectively, as shown in Fig.1.

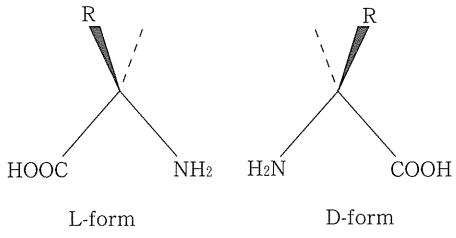


α-amino acid

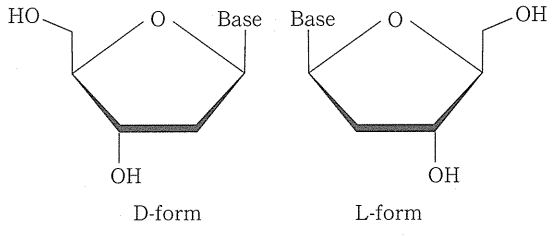


2-deoxyribose

Fig.1 Enantiomers of α-amino acid and ribose

The chemical natures, such as melting points and chemical reactivity of the enantiomers are generally the same. However, molecular chirality has an essential role in life. For example, the L-form of monosodium glutamate is used as a

seasoning of food or a delicious essence. On the other hand, the D-form of the monosodium glutamate tastes rather bitter. The role of the mirror imaged forms of the above-mentioned amino acids and riboses (5-membered sugar) have not been well understood. There is a hypothetical explanation that the isomerization or racemization of the L-form amino acids to the D-form in protein causes a serious disease. For example, there is a report that the $\beta$-amyloid partially racemized in brain attacks hippocampus, which causes Alzheimer's disease[1].

Great attention has been paid on the possible origin of the chirality, but we have not yet reached to the final answer. Recently, some of the in vitro systems are found which promote an asymmetric autocatalytic reaction by applying an organic chemical method, and are expected as the possible system for amplifying the enantiomeric imbalance starting from a trace amount of chiral initiator with very low enantiomeric excess (ee)[2]. Of course the chiral synthesis is a major and developing field of organic chemistry, and the scientific society of Japan has a very strong basis of this field as shown by the 2001 Nobel prize for chemistry given to Prof. Noyori.

There is a report which states that the sun light in the morning is left circularly polarized, whereas the sun light in the afternoon is right circularly polarized[3]. The study on photoinduced racemization is becoming an attractive field of molecular chirality, although the source of the light is such a high power like laser and far from the natural light.

Under the scientific background described above, we started a study of detection of chiral molecules by a vibrational circular dichroism (VCD) spectrometer in 2000. The purpose of our study is to observe VCD spectra of some fundamental importance in detail and clarify the relation of the VCD spectrum with molecular structure, and hopefully to find out some predictive theory to combine the VCD spectrum and dynamic property of molecular motion. This paper reviews the theoretical basis of the circular dichroism briefly and reports our preliminary results of the experimental work on the typical ring compound and aminoalcohol molecule. The ring compound was chosen to verify the quality of the *ab initio* MO calculation, and aminoalcohol molecule was chosen to investigate the molecular structure in solution, particularly the dynamic properties relating to the hydrogen bonding.

## 1. What is Circularly Polarized Light

The electromagnetic wave (hereafter the word "light" will be used to mean the electromagnetic wave) passes through material by interacting with the electromagnetic field of the atoms or molecules that constitute the material. That is why the speed of light is reduced in material of high density, although the

frequency is not changed. The speed down of the light appears as the refraction at the interface of different materials. The speed of light $c$ in a material is related with the refractive index $n$ as follows,

$$c=\frac{c_0}{n}. \qquad 1\text{-}1)$$

Where $c_0$ is the speed of light in vacuum.

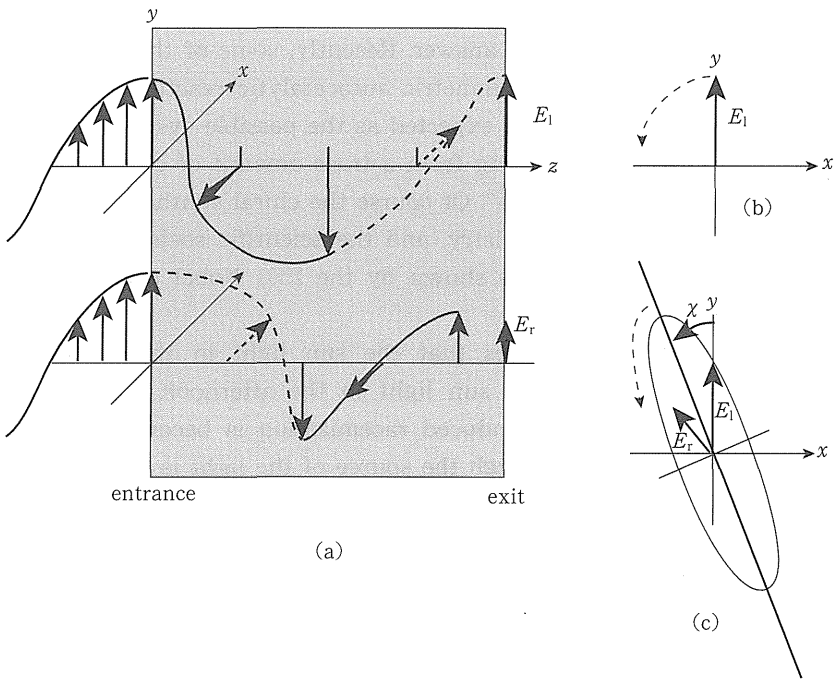


Fig.2 Circularly polarized light and elliptically polarized light

We now consider the mechanism of the rotation of polarized of light. We investigate a linearly polarized light (hereafter abbreviated as LPL) oscillating along the $y$-axis and entering into a medium (indicated by a gray zone), and propagating along the $z$-axis as shown in Fig.2(a). LPL can be considered as the sum of left and right circularly polarized lights. The left circularly polarization is defined such that the electric field is rotated anti-clockwise when we look back the light along the direction of propagation as shown in Fig.2(b). We should pay attention that when we say the rotation of the electric field, which means the rotation as the function of time. The curved line of the electric field shown in Fig.2(a) is not the wave at some particular time, but shows the electric vector experienced in the medium against the time course. In other word, the $z$-axis also means the dimension of time.

Let the linearly polarized light along the y-axis enter some medium. And Let the speeds of light of left and right circularly polarized lights to be $c_l$ and $c_r$ ($c_l > c_r$), respectively. The left circularly polarized light (denoted as LCL hereafter) passes the medium and reaches the exit faster than the right circularly polarized light (denoted as RCL hereafter). As shown in Fig.2(a), the time difference between the two polarized lights to run through the medium of length $l$ is

$$t_d = l\left(\frac{1}{c_r} - \frac{1}{c_l}\right). \tag{1-2}$$

Therefore, RCL that interferes with LCL at the exit of the medium should enter the medium before LCL by the time of $t_d$. That means the interference at the exit occurs between LCL and RCL with a phase difference of

$$\varphi = 2\pi\nu t_d = 2\pi\nu l\left(\frac{1}{c_r} - \frac{1}{c_l}\right) \tag{1-3}$$

where $\nu$ is the frequency of the light. The phase of RCL has proceeded faster then that of LCL.

The electromagnetic wave has the following fundamental relation,

$$c = \lambda\nu \tag{1-4}$$

Then, equation 1-3) can be rewritten using the above relation as follows,

$$\varphi = 2\pi\nu l\left(\frac{1}{c_r} - \frac{1}{c_l}\right) = \frac{2\pi l}{\lambda}\ (n_r - n_l). \tag{1-5}$$

If the amplitudes of the both LCL and RCL have not changed at the exit, the interference of LCL and RCL makes the polarization axis declined as much as

$$\chi = \varphi/2 \tag{1-6}$$

as shown in Fig.2(c). The optical rotation is thus explained. The angle $\alpha$ is called the angle of rotation. Equation 1-5) also explains that we have a levorotatory ($\chi < 0$, left rotation) when $c_l > c_r$, and dextrorotatory (right rotation) when $c_l < c_r$.

The difference of $c_l$ and $c_r$ should be reflected on the different absorption efficiencies for both circularly polarized lights. That is, the amplitudes of LCL and RCL should be different at the exit of the medium. Then the polarization axis has to be rotated by time, since the speeds of $E_l$ and $E_r$ are different. In case of $c_l > c_r$, the axis of polarization, or the vector addition of $E_l$ and $E_r$ should rotate anti-clockwise. In conclusion, we have the elliptic polarization as shown in Fig. 2(c).

## 2. Naming of Optically Active Molecule

Historically, the absolute configuration of optically active glyceraldehyde had

been assumed as shown in Fig.3 and the isomers of any other compounds that are synthesized starting from L-form glyceraldehyde have been denoted as L and those from D-form glyceraldehyde have been denoted as D. The symbols L and D stem from levo (left) and dextro (right) in Latin. Therefore, the symbols L and D had no relation with the real direction of optical rotation.

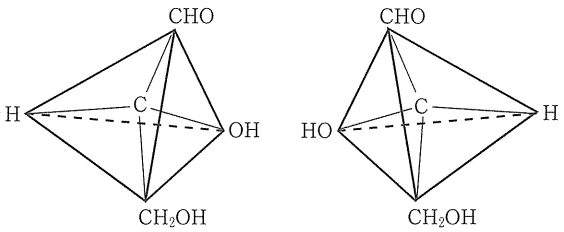


Fig.3 Absolute configuration of glyceraldehyde molecule

More convenient and logical way to express the chiral isomers was proposed by R. S. Cahn, C. K. Ingold, and V. Prelog in 1956, and now used in wide community of chemistry. The rules are made of four steps as follow. Step-1: The sequence rule to determine the relative priority is defined for four atoms or groups connected to the chiral center. Step-2: Put the atom or group of the lowest priority among them behind the chiral center, and look the remaining three at the front of the chiral center. Step-3: The three atoms or groups are looped according to the sequence order. Step-4: If the loop is right turn, the chiral isomer is called *R* (rectus: straight or right in Latin), and if the loop is left turn, the isomer is call *S* (sinister: left in Latin).

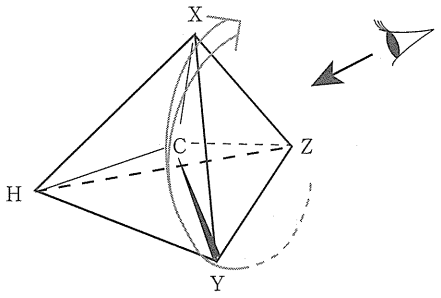


Fig.4 *R, S* - Representation of optically active molecule

The sequence rules are defined as follows:

Rule-1: If the four atoms connected to the chiral center are different, the priority follows the atomic number. The atom with larger atomic number is assigned the higher priority. If two atoms are the same element, the isomer with larger mass number is assigned the higher priority.

Rule-2: If the sequence order cannot be determined by the rule-1, we compare the atoms next to the first substituents. If necessary, the same procedure is repeated.

Rule-3: If we met a double or triple bond, we count the atoms of both side of themultiple bond, doubly or triply. For example, we assume $>C=A$ by $\begin{matrix} >C-A, \\ \quad\ \ | \quad | \\ \quad\ A \quad C \end{matrix}$ and $-C\equiv A$ by $\begin{matrix} \quad A \quad C \\ \quad\ | \quad\ | \\ -C-A. \\ \quad\ | \quad\ | \\ \quad A \quad C \end{matrix}$ The phenyl group, $C_6H_5-$, is treated as one of the Kekele structures.

The D-glyceraldehyde is now assigned to *R* chiral isomer, and L-glyceraldehyde is to *S* isomer as shown in Fig.4.

## 3. What is Circular Dichroism

Circular dichroism (CD) accompanying the electronic transition has been used as a sensitive method to detect the optical active molecules. Many theories to explain the optical rotation and CD have been proposed and successfully applied for extensive chemical systems. We summarized the most general theories of CD in the following sections.

### 3-1. Electromagnetic Explanation

First we introduce two classical theories depending on the electromagnetism.

3-1-1. Kuhn's Theory

Kuhn assumed two oscillators, $\mu_1$ and $\mu_2$, separated by some distance, say $d$, in an asymmetric molecule. That is, two oscillators are coupled and make two orthogonal motions or normal modes. Here we take $\xi_1=(\mu_1+\mu_2)$ and $\xi_2=(\mu_1-\mu_2)$ as a model as shown in Fig.5(a) and (b), where the normalization coefficients are ignored for simplicity.

We next consider the interaction of the mode $\xi_1$ with electromagnetic wave. Fig.5(c) and (d) show the case when the two oscillators are separated by $\lambda/4$. Take the case when the first oscillator $\mu_1$ is accelerated by the incident lights, LCL and RCL. The oscillator $\mu_1$ of the mode $\xi_1$ will stimulate the motion of the oscillator $\mu_2$ as shown in the figure. When the LCL reached the position of $\mu_2$, the photon of LCL may be absorbed strongly since the directions of electric vector and dipole moment of $\mu_2$ are in coincidence. Whereas, the directions of electric vector of RCL and dipole moment of $\mu_2$ are reversed, and the absorption of the

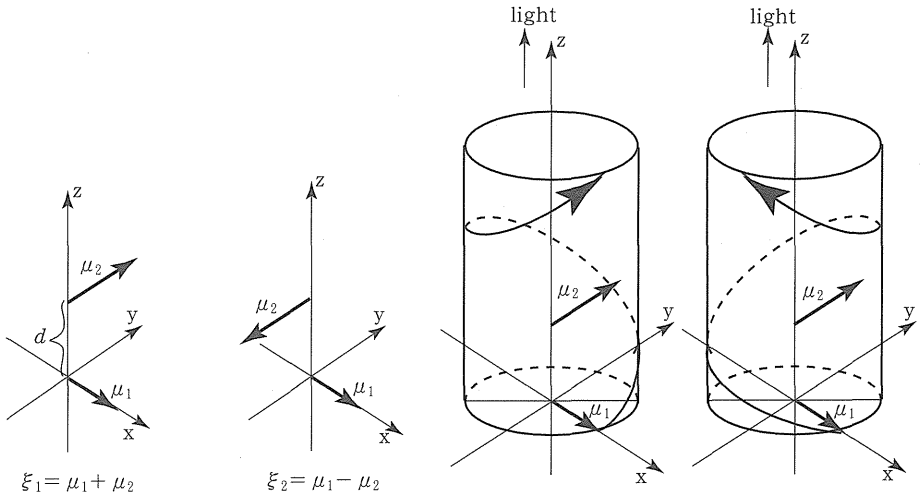


Fig.5 Coupled oscillator model

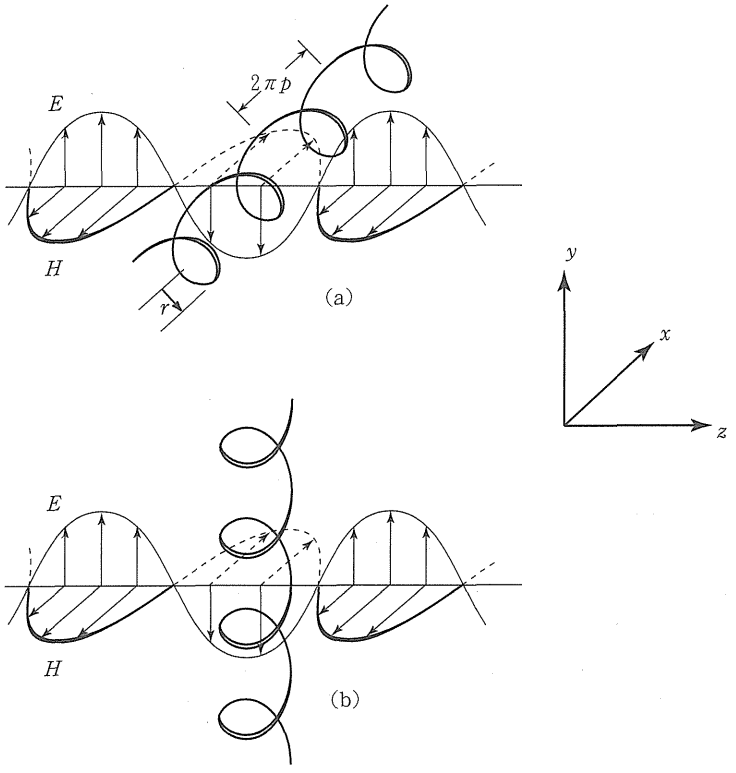


Fig.6 Spiral model

photon may be depressed compared to the case of LCL.

According to Kuhn's theory, there needs more than two oscillators in a molecule, and these oscillators should be separated by some distance and should not be on the same plane nor in parallel.

### 3-1-2. One Electron Theory

According to Kuhn's model described above, the circular dichroism occurs by the difference of the light absorptions for LCL and RCL, which makes the phase difference for both circularly polarized lights as described in section 1. On the other hand, we can make a model where the circularly polarized light is a combination of the two linearly polarized lights, orthogonal in their electric fields and shifted by 90° in its phase. In return for the assumption of the linearly polarization of electromagnetic wave, we need to introduce some mechanism where the electric charges move in spiral in a molecule to cause the circular dichroism.

Let's assume some molecule to have a spiral structure in it. In Fig. 6, a right spiral is shown which is placed along the $x$-axis and the electromagnetic wave propagates from left to right along the $z$-axis with the electric field, $E$, linearly polarized along the $y$-axis and the magnetic field, $H$, is perpendicular to $E$. The radius of the spiral is $r$. The charge of the molecule is forced to move along the spiral. By the incident light, there induced the electric and magnetic dipole moments ($\mu$, $m$), given by the derivative of time($t$) as the following equations,

$$\mu = -\left(\frac{\beta}{c}\right)\frac{\partial H}{\partial t} \qquad 3\text{-}1)$$

$$m = +\left(\frac{\beta}{c}\right)\frac{\partial E}{\partial t} \qquad 3\text{-}2)$$

where $c$ is the speed of light and $\beta$ is a constant depending on the molecule. First, we consider the induced electric dipole moment given by equation 3-1). Two components, $\mu_x$ and $\mu_{yz}$, will be induced. The former one is along the spiral axis, and the latter one is perpendicular to the spiral axis. By one turn of the charge, the sum of $\mu_{yz}$ becomes zero, but $\mu_x$ sums up to be $2\pi ep$, where $p$ is the distance that the spiral proceeds along the axis per unit angle (radian), and $e$ is the unit charge. Therefore, we only need to consider $\mu_x$. The induced electric dipole moments will oscillate with the same frequency of the incident light.

According the electromagnetism, the oscillating charge will induce the electromagnetic wave. In our case, the emitted light is polarized along the $x$-axis. The incident light and induced light will make a combined electric field which is declined by $\chi$ from the electric field of the incident light as shown in Fig. 7.

Let's calculate the induced electric dipole moment. The magnetic field of the

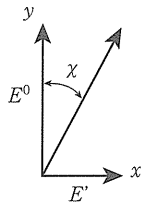


Fig.7 Vector addition of incident and induced electric fields

incident light can be written by

$$H=-H_0\cos\omega\left(t-\frac{z}{c}\right). \tag{3-3}$$

Then, equation 3-1) is rewritten by incorporating equation 3-3) as

$$\mu=\mu_x=-\frac{\beta}{c}\dot{H}=-\frac{\beta}{c}\frac{n^2+2}{3}\omega H_0\sin\omega\left(t-\frac{z}{c}\right). \tag{3-4}$$

The amount of the electric vector $E$ emitted from the dipole moment expressed by equation 3-4) will be derived to be

$$|E_x^{\mu}|=N\mu_x=\frac{4\pi^2N}{\lambda}\mathrm{d}z\ \frac{n^2+2}{3}\cdot\frac{\beta}{c}|H_0|\cos\omega\left(t-\frac{z}{c}\right) \tag{3-5}$$

where $N$ is the number of molecules per unit volume of the medium.

The electric field can induce a magnetic moment as written in equation 3-2). In this case, we use a model shown in Fig.6(b). The electric field of the incident light induce the movement of charge in the spiral (actually molecule) placed along the $y$-axis, which in turn induce a magnetic moment along the $y$-axis, $m_y$. The oscillation of this magnetic moment produces the electric feield perpendicularly to the magnetic moment, which is along the $x$-axis. The arithmetic will follow as those described above for the induced electric dipole moment, and we obtain the same amount of the electric field, $|E_x^m|$ as equation 3-5)

In a real medium, the directions of molecules are randomly distributed and we need to sum up or integrate all of the contributions and average them according to the recipe of kinetic model of the gas phase molecules. The result is just simple so that the averaged electric field stimulated by the incident light is one third of the sum of $|E_x^{\mu}|$ and $|E_x^m|$. In conclusion, we have

$$E'=\frac{1}{3}[|E_x^{\mu}|+|E_x^m|]=\frac{8\pi^3N}{3\lambda}\mathrm{d}z\ \frac{n^2+2}{3}\cdot\frac{2\beta}{c}|E^0| \tag{3-6}$$

where $|E^0|$is the electric field of the incident light. As is shown in Fig.7, the polarization degree, $\chi$, is related with $|E'|$and $|E^0|$ by the following relation.

$$\chi\approx\tan\chi=\frac{|E'|}{|E^0|}=\frac{8\pi^3N}{3\lambda^2}\mathrm{d}z\ \frac{n^2+2}{3}2\beta. \tag{3-7}$$

3-1-3. Derivation of $\beta$

There are three kinds of forces that interact with the charge (we will treat an electron as a typical charge) on the spiral shown in Fig.6. Those are 1) force, $f_i$, accompanying to the acceleration of the electron motion, 2) Hooke's force, $f_b$, against to the displacement of the electron, and 3) force by the magnetic field of the incident light, $f_e$. These forces should be in balance. The first two forces are related with the displacement, $q$, of the electron along the spiral by the following equations,

$$f_i = -m\ddot{q}, \tag{3-8}$$

$$f_b = -kq. \tag{3-9}$$

Potential difference for one turn of the spiral, caused by the magnetic field, is

$$\Delta V = \left(\pi r^2 / c\right) |\dot{H}|. \tag{3-10}$$

Since the length of one turn of the spiral is $2\pi\sqrt{r^2+p^2}$, the potential difference for a unit of $q$ is

$$|V| = \frac{\Delta V}{2\pi\sqrt{r^2+p^2}} = \frac{r^2}{2c\sqrt{r^2+p^2}}|\dot{H}|. \tag{3-11}$$

Therefore, the force, $f_e$, derived by this potential difference is

$$f_e = e|V| = \frac{er^2}{2c\sqrt{r^2+p^2}}|\dot{H}|. \tag{3-12}$$

The balance of three forces in equations, 3-8), 3-9), and 3-12) is described by

$$m\ddot{q} + kq + \frac{er^2}{2c\sqrt{r^2+p^2}}|\dot{H}| = 0. \tag{3-13}$$

By introducing the relations, $H = \omega H_0 \sin\omega t$ and $k = m\omega_0^2$, into the above equation, we will obtain the next solution for $q$, as

$$q_0 = -\frac{er^2}{2mc\sqrt{r^2+p^2}} \cdot \frac{1}{\omega_0^2 - \omega^2}\omega |H_0| \sin\omega t. \tag{3-14}$$

The $x$-component of $q_0$ is $q_0 p / \sqrt{r^2+p^2}$, so that the electric dipole moment $\mu_x$ along the $x$-axis caused by the displacement of $q_0$ is

$$\mu_x = \frac{2q_0 pe}{\sqrt{r^2+p^2}} = -\frac{e}{mc} \cdot \frac{r^2 p}{r^2+p^2} \cdot \frac{1}{\omega_0^2 - \omega^2}\dot{H}. \tag{3-15}$$

Comparing this equation with that of 3-1), we obtain

$$\beta = \frac{e^2}{m} \cdot \frac{r^2 p}{r^2+p^2} \cdot \frac{1}{\omega_0^2 - \omega^2}. \tag{3-16}$$

By assigning this relation into equation 3-7), we can derive the next formula,

$$\chi=\frac{16\pi^3 N}{3\lambda^2}\mathrm{d}z\ \frac{n^2+2}{3}\cdot\frac{e^2}{m}\cdot\frac{r^2 p}{r^2+p^2}\cdot\frac{1}{\omega_0^2-\omega^2}. \qquad 3\text{-}17)$$

Experimentally, we use a specific rotation, $[\alpha]$, defined as the optical rotation for the concentration 1 g/ml, and for the optical length of 1 dm. In the case of the concentration of $[c]$ (g/ml) and the optical length of $\mathrm{d}z$ (cm), $[\alpha]$ will be described as follows,

$$[\alpha]=\frac{180\chi}{\pi}\cdot\frac{10}{\mathrm{d}z}\cdot\frac{1}{[c]}, \qquad 3\text{-}18)$$

where $[\alpha]$ is expressed by the degree, $\chi$ by radian, $[c]$ by the weight of solute in 1 ml solution. Here we introduce the Avogadro constant, $N_A$, and molecular weight, $M$. Then, $N$ in equation 3-17) is expressed by $N=N_A[c]/M$. Assigning this relation and $\omega=2\pi c/\lambda$, and equation 3-17) into 3-18), we obtain

$$[\alpha]=2400\frac{N_A}{M}\cdot\frac{n^2+2}{3}\cdot\frac{e^2}{mc^2}\cdot\frac{r^2 p}{r^2+p^2}\cdot\frac{\lambda_0^2}{\lambda^2-\lambda_0^2}. \qquad 3\text{-}19)$$

By replacing some parts of the above formula, like

$$a_0=24N_A\frac{e^2}{mc^2}\cdot\frac{r^2 p}{r^2+p^2}, \qquad 3\text{-}20)$$

we obtain a simplified formula for the specific rotation as follows,

$$[\alpha]=\frac{100}{M}\cdot\frac{n^2+2}{3}\cdot\frac{a_0\lambda_0^2}{\lambda^2-\lambda_0^2}. \qquad 3\text{-}21)$$

From equation 3-19) or 3-21), we can deduce some important results. In the wave length region of $\lambda>\lambda_0$, the sign of $[\alpha]$ is determined only by the sign of $p$. The positive sign of $p$ means that the spiral is right turn, and the negative sign means left turn. The equation 3-21) explains the anomalous dispersion observed in CD spectrum of the electric transition and $\lambda_0$ corresponds to the absorption wavelength where the so-called Cotton effect appears.

From equation 3-19) or 3-21), we can deduce another conclusion. That is, for the spectrum to be optically active, $r$ and $p$ should not be zero. The zero value of $r$ corresponds to the case when the charge in molecule oscillates on the straight line, whereas the zero value of $p$ corresponds to the case when the charge in molecule oscillates in a closed circuit.

The formula of 3-20) can be divided into two parts, except the coefficient such as

$$a_0=24N_A\frac{1}{mc^2}\cdot\frac{ep}{\sqrt{r^2+p^2}}\cdot\frac{er^2}{\sqrt{r^2+p^2}}. \qquad 3\text{-}22)$$

The multiplication of the second part of the above equation with $q_0$ is an induced electric dipole moment as is indicated by 3-15), and the third part of the equation is in proportion to the induced magnetic moment. Therefore, we de-

duced the conclusion that the optical activity needs nonzero induced electric moment and nonzero induced magnetic moment accompanying the optical absorption. Equation 3-22) tells that $p=0$ means zero value of the induced electric dipole moment and $r=0$ means zero value of the induced magnetic dipole moment.

## 3-2. Quantum Mechanical Explanation

We have derived the explanation for the optical activity of the molecule from the classical electromagnetism in the preceding section. Here we will try to explain the optical activity by the quantum mechanical point of view and correlate it with that of the electromagnetism.

Time-dependent Schrödinger equation for a system characterized by the state, $n$, with the wavefunction $\Psi_n^0(t)$ and the energy $E_n^0$ is

$$H_0\Psi_n^0(t)=i\hbar\frac{\partial}{\partial t}\Psi_n^0(t)=E_n^0\Psi_n^0(t). \tag{3-23}$$

The wavefunction $\Psi_n^0(t)$ can be divided into two parts as

$$\Psi_n^0(t)=\Psi_n^0\exp(-i\frac{E_n^0}{\hbar}t), \tag{3-24}$$

where $\Psi_n^0$ is the time-independent wavefunction of space variables. Let us consider a new state $k$, where the molecule is under influence of a dynamic field perturbation, and assume that the perturbation is weak. Then the total Hamiltonian $H(t)$ can be written as

$$H(t)=H_0+H_1(t). \tag{3-25}$$

We will treat only the first order perturbation here. Since $\Psi_n^0(t)$ constitutes a complete system, the wavefunction $\Psi_k(t)$ can be expanded as a Fourier series of $\Psi_n^0(t)$ as follows,

$$\Psi_k(t)=\sum c_n(t)\Psi_n^0(t). \tag{3-26}$$

By incorporating equations 3-25) and 3-26) into the general form of the Schroedinger equation, $H(t)\Psi_k(t)=i\hbar\frac{\partial}{\partial t}\Psi_k(t)$, we obtain the time-dependent equation as follows,

$$\{H_0+H_1(t)\}\sum c_n(t)\Psi_n^0(t)=i\hbar\frac{\partial}{\partial t}\sum c_n(t)\Psi_n^0(t). \tag{3-27}$$

By expanding this equation using $H_0\Psi_n^0(t)=E_n^0\Psi_n^0(t)$ and $\Psi_n^0(t)=\Psi_n^0\exp(-i\frac{E_n^0}{\hbar}t)$, and by left multiplying with $\Psi_k^{0*}$, we obtain the next equation,

$$\frac{\partial c_k(t)}{\partial t}=\frac{1}{i\hbar}\sum c_n(t)\langle\Psi_k^0|H_1(t)|\Psi_n^0\rangle\exp\left\{\frac{-i(E_n^0-E_k^0)t}{\hbar}\right\}. \tag{3-28}$$

Suppose that the system was in the state, $s$, initially. Then the coefficients

should be

$$c_s(0)=1,\ c_n(0)=0 \qquad (n\neq s). \tag{3-29}$$

We can assume that the coefficient at time $t$, $c_s(t)$, is close to 1, and the other coefficients $c_n(t)(n\neq s)$ are very small. Then, the coefficients $c_n(t)$ can be written as

$$c_n(t)=\frac{1}{i\hbar}\int \langle \Psi_n^0|H_1(t)|\Psi_s^0\rangle e^{i\omega_{ns}t}dt, \tag{3-30}$$

where

$$\omega_{ns}=\frac{E_n^0-E_s^0}{\hbar}. \tag{3-31}$$

Now let's consider the system that is perturbed by the dynamic electric field. The perturbing Hamiltonian can be expressed as

$$H_1(t)=-\mu_\alpha E_\alpha(t). \tag{3-32}$$

And the perturbing Hamiltonian for the system perturbed by the dynamic magnetic field can be expressed as (In the preceding two sections, we used $H$ for the magnetic field, but we will use the symbol $B$ for the magnetic filed hereafter to avoid the confusion of the Hamiltonian $H$ and the magnetic field)

$$H_1(t) = -m_\alpha B_\alpha(t). \tag{3-33}$$

We next examine the system that is perturbed by the circularly polarized light. Assume that the light propagates along the $z$-axis, the circularly polarized electric vector $\boldsymbol{E}^{\pm}(t)$ will be expressed by

$$\boldsymbol{E}^{\pm}(t)=2E_0\left\{\boldsymbol{u}\cos\omega\left(t-\frac{z}{c}\right)\pm\boldsymbol{v}\sin\omega\left(t-\frac{z}{c}\right)\right\}, \tag{3-34}$$

where the left and right circularly polarized lights are represented by "+" and "−" signs, respectively under the right-handed coordinates system, and $\boldsymbol{u}$ and $\boldsymbol{v}$ represent unit vectors along the $x$- and $y$-axes, respectively. The corresponding magnetic vector $\boldsymbol{B}^{\pm}(t)$ can be obtained by rotating $\boldsymbol{E}^{\pm}(t)$ around the $z$-axis by $\frac{\pi}{2}$, so that

$$\boldsymbol{B}^{\pm}(t)=2B_0\left\{\mp\boldsymbol{u}\sin\omega\left(t-\frac{z}{c}\right)+\boldsymbol{v}\cos\omega\left(t-\frac{z}{c}\right)\right\}. \tag{3-35}$$

Both $\boldsymbol{E}^{\pm}(t)$ and $\boldsymbol{B}^{\pm}(t)$ have only the $x$- and $y$- components, and then the perturbing Hamiltonian will be written by

$$H_1^{\pm}(t)=-\mu_x E_x^{\pm}(t)-\mu_y E_y^{\pm}(t)-m_x B_x^{\pm}(t)-m_y B_y^{\pm}(t). \tag{3-36}$$

From equations 3-34) and 3-35), the $x$- and $y$- components of $\boldsymbol{E}^{\pm}(t)$ and $\boldsymbol{B}^{\pm}(t)$ are deduced to be

$$E_x^{\pm}(t)=2E_0\cos\omega\left(t-\frac{z}{c}\right),\quad E_y^{\pm}(t)=\pm 2E_0\sin\omega\left(t-\frac{z}{c}\right), \tag{3-37}$$

$$B_x^{\pm}(t)=\mp 2B_0\sin\omega\left(t-\frac{z}{c}\right),\quad B_y^{\pm}(t)=2B_0\cos\omega\left(t-\frac{z}{c}\right). \tag{3-38}$$

In these equations, the phase difference $\omega\frac{z}{c}$ is in common, so that we can omit this term in the following discussions. By assigning these equations into 3-36), the perturbing Hamiltonian will be written by

$$\begin{aligned}H_1^{\pm}(t)=&E_0\{-\mu_x(e^{i\omega t}+e^{-i\omega t})\pm i\mu_y(e^{i\omega t}-e^{-i\omega t})\}\\&+B_0\{\mp im_x(e^{i\omega t}-e^{-i\omega t})-m_y(e^{i\omega t}+e^{-i\omega t})\}\end{aligned}. \tag{3-39}$$

Then the equation 3-30) is rewritten as

$$c_n^{\pm}(t)=\frac{1}{i\hbar}\begin{Bmatrix}(-E_0\mu_{x,\,ns}-B_0m_{y,\,ns})\int(e^{i\omega t}+e^{-i\omega t})e^{i\omega_{ns}t}dt\\\pm i(E_0\mu_{y,\,ns}-B_0m_{x,\,ns})\int(e^{i\omega t}-e^{-i\omega t})e^{i\omega_{ns}t}dt\end{Bmatrix}, \tag{3-40}$$

where, $\mu_{x,\,ns}=\langle\Psi_n^0|\mu_x|\Psi_s^0\rangle$, and so on.

The effect of the $(e^{i\omega t}\pm e^{-i\omega t})$ term in the perturbing Hamiltonian on the coefficients $c_n^{\pm}(t)$ results in the integration $\int(e^{i\omega t}\pm e^{-i\omega t})e^{i\omega_{ns}t}dt$. By calculating this integration, the following equation can be derived.

$$\int(e^{i\omega t}\pm e^{-i\omega t})e^{i\omega_{ns}t}dt=\frac{e^{i(\omega_{ns}+\omega)t}-1}{i(\omega_{ns}+\omega)}\pm\frac{e^{i(\omega_{ns}-\omega)t}-1}{i(\omega_{ns}-\omega)}. \tag{3-41}$$

Next we will discuss about the absorption phenomenon. Since the first term of the right hand side of equation 3-41) is negligible, this equation can be rewritten as

$$\int(e^{i\omega t}\pm e^{-i\omega t})e^{i\omega_{ns}t}dt=\pm\frac{e^{i(\omega_{ns}-\omega)t}-1}{i(\omega_{ns}-\omega)}. \tag{3-42}$$

Then equation 3-40) becomes

$$\begin{aligned}c_n^{\pm}(t)=&\frac{1}{i\hbar}(-\mu_{x,\,ns}E_0\mp i\mu_{y,\,ns}E_0\pm im_{x,\,ns}B_0-m_{y,\,ns}B_0)\frac{e^{i(\omega_{ns}-\omega)t}-1}{i(\omega_{ns}-\omega)}\\=&-\frac{V_{1,ns}^{\pm}(e^{i(\omega_{ns}-\omega)t}-1)}{\hbar(\omega_{ns}-\omega)},\end{aligned} \tag{3-43}$$

where

$$V_{1,\,ns}^{\pm}=-\mu_{x,\,ns}E_0\mp i\mu_{y,\,ns}E_0\pm im_{x,\,ns}B_0-m_{y,\,ns}B_0 \tag{3-44}$$

The probability $P_n^{\pm}(t)$ of finding the molecule in the state $n$ can be derived as

$$\begin{aligned}P_n^{\pm}(t)=&\{c_n^{\pm}(t)\}\{c_n^{\pm}(t)\}^*\\=&\frac{4V_{1,\,ns}^{\pm}(V_{1,\,ns}^{\pm})^*\sin^2\frac{1}{2}(\omega_{ns}-\omega)t}{\hbar^2(\omega_{ns}-\omega)^2}.\end{aligned} \tag{3-45}$$

By taking the hermiticity of $\mu_\alpha$ and $m_\alpha$ into consideration, we can obtain

$$\begin{aligned} V^{\pm}_{1,ns}(V^{\pm}_{1,ns})^* &= (\mu_{x,sn}\mu_{x,ns}+\mu_{y,sn}\mu_{y,ns})E_0^2 \\ &+(m_{x,sn}m_{x,ns}+m_{y,sn}m_{y,ns})B_0^2 \\ &\mp 2\mathrm{i}(\mu_{x,sn}m_{x,ns}+\mu_{y,sn}m_{y,ns})E_0B_0 \end{aligned} \quad . \tag{3-46}$$

For an isotropic sample, all directions of space cannot be discriminated. Therefore, every component is summed up and the equation can be rewritten as

$$V^{\pm}_{1,ns}(V^{\pm}_{1,ns})^* = \frac{2}{3}\{\mu_{\alpha,sn}\mu_{\alpha,ns}E_0^2+m_{\alpha,sn}m_{\alpha,ns}B_0^2 \pm 2\mathrm{Im}(\mu_{\alpha,sn}m_{\alpha,ns})E_0B_0\}, \tag{3-47}$$

where, Einstein summation convention, $a_\alpha b_\alpha = a_x b_x + a_y b_y + a_z b_z$, is applied.

The $E_0^2$, $B_0^2$, $E_0B_0$ terms in equation 3-46) can be converted to the energy of the incident light. We now need to integrate $P_n^{\pm}(t)$ over all the quantum states in the incident energy range, and differentiate it by $t$ to derive $W^{\pm}$, the transition rate per a unit time. The result is

$$\begin{aligned} W^{\pm} &= \frac{8\pi^3}{3h^2}\{\mu_{\alpha,sn}\mu_{\alpha,ns}+m_{\alpha,sn}m_{\alpha,ns} \pm 2\mathrm{Im}(\mu_{\alpha,sn}m_{\alpha,ns})\}\rho(\nu) \\ &= \frac{8\pi^3}{3h^2}\{\boldsymbol{\mu}_{sn}\cdot\boldsymbol{\mu}_{ns}+\boldsymbol{m}_{sn}\cdot\boldsymbol{m}_{ns} \pm 2\mathrm{Im}(\boldsymbol{\mu}_{sn}\cdot\boldsymbol{m}_{ns})\}\rho(\nu) \end{aligned} \quad , \tag{3-48}$$

where $\rho(\nu)$ is the energy density (energy per volume per Hz).

Now let's assume that the sample with the concentration $C_0$ absorbs a photon of the energy $h\nu$ from the incident light with intensity of $I(\nu)$. The change in the intensity of light is proportional to the thickness of the sample, or the optical path length $l$. Assume that the energy difference between the states $s$ and $n$ in equation 3-48) is large enough, and all the molecules are in the state $s$ initially. Then, by using the relation $I(\nu)=c\rho(\nu)$, we can derive

$$\left(\frac{\mathrm{d}I(\nu)}{I(\nu)}\right)^{\pm} = \left(\frac{B^{\pm}}{c}\right)h\nu C_0 N_A \mathrm{d}l, \tag{3-49}$$

where $N_A$ is the Avogadro number, and $B^{\pm}$ can be written as

$$B^{\pm} = \frac{8\pi^3}{3h^2}\{\boldsymbol{\mu}_{sn}\cdot\boldsymbol{\mu}_{ns}+\boldsymbol{m}_{sn}\cdot\boldsymbol{m}_{ns} \pm 2\mathrm{Im}\ (\boldsymbol{\mu}_{sn}\cdot\boldsymbol{m}_{ns})\}. \tag{3-50}$$

In case of the ordinary absorption, only $\mu_{\alpha,sn}\mu_{\alpha,ns}$ term in equation 3-50) is needed, so that we obtain

$$\ln\frac{I_0(\nu)}{I(\nu)} = \frac{8\pi^3\nu C_0 N_A l}{3hc}D_{ns}, \tag{3-51}$$

where $I_0(\nu)$ represents the intensity of light at the entrance of the sample. The term $D_{ns}$ represents the electric-dipole transition strength, which satisfies the relation of

$$D_{ns}=\mu_{\alpha,sn}\mu_{\alpha,ns}=\boldsymbol{\mu}_{sn}\cdot\boldsymbol{\mu}_{ns}. \tag{3-52}$$

By using $\alpha(\nu)$, the absorption coefficient, the Lambert-Beer's law can be written as

$$I(\nu)=I_0(\nu)e^{-\alpha(\nu)C_0 l}. \tag{3-53}$$

From equations 3-50) and 3-53), we obtain the following relation,

$$\alpha(\nu)=\frac{8\pi^3\nu N_A}{3hc}D_{ns}. \tag{3-54}$$

For the purpose to obtain the total absorption intensity of the spectral band, we need to calculate $\int\frac{\alpha(\nu)}{\nu}d\nu$ by taking the band shape into the consideration. Actually, the variation of the frequency $\nu$ is limited over the spectral band, we can replace $\nu$ by $\nu_0$, the frequency of the band center. Then, the integration becomes

$$a=\int\alpha(\nu)d\nu=\frac{8\pi^3\nu_0 N_A}{3hc}D_{ns}. \tag{3-55}$$

We now investigate the circular dichroism intensities. The equation corresponding to 3-51) can be written as

$$\ln\frac{I_0(\nu)}{I(\nu)}=\frac{8\pi^3\nu C_0 N_A l}{3hc}(D_{ns}+M_{ns}\pm 2R_{ns}), \tag{3-56}$$

where

$$M_{ns}=m_{\alpha,sn}m_{\alpha,ns}=\boldsymbol{m}_{sn}\cdot\boldsymbol{m}_{ns}, \tag{3-57}$$

and

$$R_{ns}=\mathrm{Im}(\mu_{\alpha,sn}m_{\alpha,ns})=\mathrm{Im}(\boldsymbol{\mu}_{sn}\cdot\boldsymbol{m}_{ns}). \tag{3-58}$$

Then the absorption coefficients $\alpha^{\pm}(\nu)$ become

$$\alpha^{\pm}(\nu)=\frac{8\pi^3\nu N_A}{3hc}(D_{ns}+M_{ns}\pm 2R_{ns}). \tag{3-59}$$

By integrating this relation over the band, the equation corresponding to 3-55) is derived as

$$a^{\pm}=\int\alpha^{\pm}(\nu)d\nu=\frac{8\pi^3\nu_0 N_A}{3hc}(D_{ns}+M_{ns}\pm 2R_{ns}). \tag{3-60}$$

Now we can obtain $\Delta a=a^{+}-a^{-}$ as

$$\Delta a=\int\{\alpha^{+}(\nu)-\alpha^{-}(\nu)\}d\nu=4\left(\frac{8\pi^3\nu_0 N_A}{3hc}\right)R_{ns}. \tag{3-61}$$

Here $R_{ns}$ is called the rotational strength, which is related to the direction and the intensity of the CD spectrum.

At this stage, we understand that a physical explanation of the optical activity

or the different reaction of the chiral molecule against LCL and RCL has been derived on the basis of quantum mechanics. The formula of 3-59) or 3-60) that is derived from quantum mechanics will be compared to the equation 3-22) that is derived from classical electromagnetism. Both formulae, 3-22) and 3-60), contain the contributions from the electric dipole transition and magnetic dipole transition, and we need nonzero value as their inner product.

The ratio $\frac{\Delta a}{a}$ is called the anisotropic factor or the dissymmetric factor, and usually written as $g$. From equations 3-55) and 3-61), $g$ is described as

$$g=\frac{\Delta a}{a}=\frac{4R_{ns}}{D_{ns}}. \qquad 3\text{-}62)$$

The $g$ value of the electronic transition in visible and ultraviolet region is in order of $10^{-2}$ to $10^{-3}$, whereas that of the vibrational transition in infrared region is in order of $10^{-4}$ to $10^{-5}$. The sensitivity of measurement in infrared region is lower than that in visible and ultraviolet region by an order of $10^{-2}$. This is why the study of vibrational circular dichroism (VCD) has been behind the experimental study on the electronic chircular dichroism (ECD).

## 4. Vibrational Optical Activity

As the infrared absorption spectroscopy and Raman scattering spectroscopy are complementary methods in vibrational spectroscopy, there are two methods that measure the vibrational optical activity (VOA). These are vibratinal circular dichroism (VCD) that measures absorption difference of the chiral molecules by the circularly polarized infrared radiations, and vibrational Raman optical activity (ROA) that measures the different features of Raman spectra using circularly polarized laser radiation.

The research on VOA started in early 1970s. The VCD instrument was constructed by Holzworth in early stage of development[5], and applied for the measurement of single crystal of $NiSO_4 \cdot 6H_2O$ in 1973[6], and then to liquid sample in 1974[7]. Since then there has been a steady development in measuring techniques and theoretical explanations. Recently, a commercial VCD and ROA instruments are available, and purely theoretical calculation method is incorporated in a widely used *ab initio* MO calculation package. There have been published a lot of references on VOA[8]. Even so, VOA methods are not well spread over the communities of analytical chemistry, chiral chemistry, pharmaceutical sciences, and so on. The reason would be that the measurement of VOA has been difficult, and only a few groups have been able to carry out the experimental researches. Therefore, the experiences on VOA spectra are still limited and we do not have enough data to elucidate some empirical rules that relate the spectral features with geometrical and/or other natures of molecules.

Any key band would be helpful even when we do not have some clear theoretical explanations of them for practical purposes, but any effort has not been paid along this line, maybe because of their experimental difficulties and limited data available.

We now have easy-to-use apparatus available commercially as described above and the theoretical tool to predict the observed VOA spectrum (at this moment, only VCD spectrum can be treated) with sufficient accuracy enough to assign the observed spectrum. The time is maturing to carry out extensive survey of the chiral molecules. This is our motivation to start the VOA, especially VCD research. We aim to experience, first, to measure some small but typical molecules in great detail and most carefully, for the evaluation of the potentiality of the VCD method.

Table 1 shows the comparison of characteristics of electronic circular dichroism (ECD) and vibrational circular dichroism (VCD). ECD has the higher sensitivity than VCD and there have been so many experiences stored in modern scientific researches. However the ECD spectrum is rather simple and broad, therefore the information from the spectrum is limited. On the contrary, VCD activity is accompanied by each vibrational mode, aside its intensity. Therefore, VCD should have so many pieces of information in essence. Although their analyses are rather difficult since there is no apparent relation between VCD strength and its direction with the corresponding infrared absorption band.

Table.1 Comparison of ECD and VCD

| | Electronic Circular Dichroism | Vibrational Circular Dichroism |
|---|---|---|
| wavelength region | ultraviolet & visible | infrared |
| transition | electronic | vibrational |
| electronic state | ground & excited | ground |
| observable | chromophore | many vibrational modes |
| sample | molecules with chromophores | not restricted |
| information | poor | rich |
| anisotropic factor | $\sim 10^{-3}$ | $10^{-4} \sim 10^{-5}$ |
| analysis | difficult | rather easy |
| sensitivity | high | low |

## 5. Method for Measuring VCD Spectrum

Fig.8 shows a block diagram of VCD apparatus. The monochromatic infrared radiation by a dispersive spectrometer or modulated infrared radiation by a Fourier transform spectrometer is introduced into a system of creation and modulation of circularly polarized light. The creation and selective detection of LCL and RCL is carried out with the combination of a polarizer and a quarter-

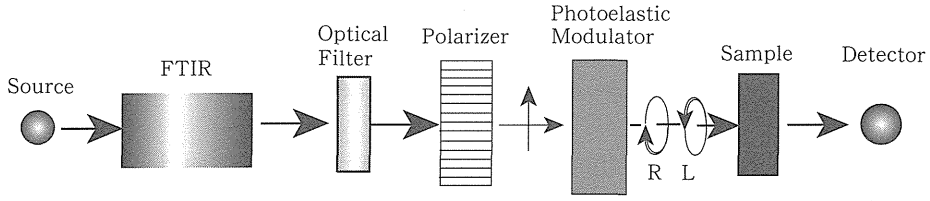


Fig.8 Block diagram of VCD spectrometer

wave plate which is modulated by an electric circuit at the frequency between 20 and 100 kHz. The polarized infrared radiation is illuminated onto the sample, and the transmitted IR is focused onto the high-sensitive IR detector, usually a liquid $N_2$ cooled MCT (HgCdTe) or InSb detector.

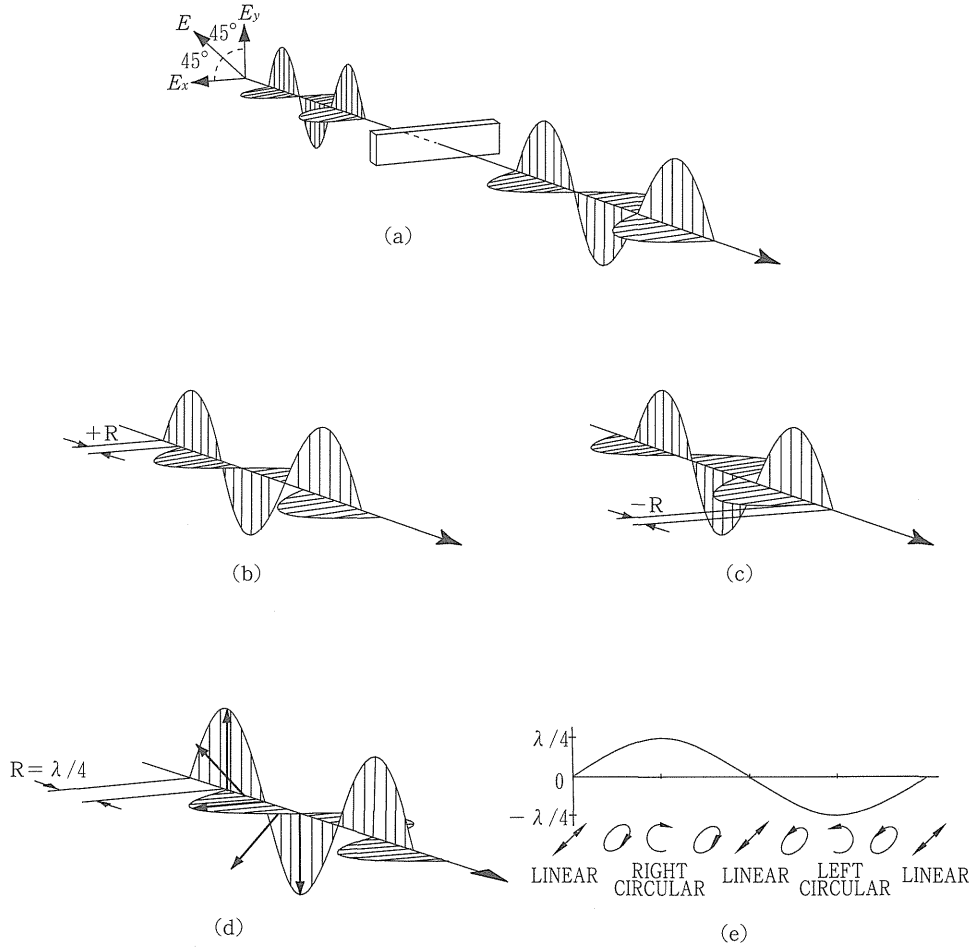


Fig.9 Retardation effects of compression and extension

### 5-1. Principle of Photoelastic Modulator

One of the most important module in VCD spectrometer should be a photoelastic modulator, PEM. PEM is a device that consists of a rectangular bar of birefringence (double refraction) material transparent for infrared radiation attached to a piezoelectric transducer. By applying the alternating current to the piezoelectric transducer, the birefringence crystal starts oscillate with its resonant frequency ($\omega_m$), which in turn produce the oscillating anisotropy of the refractive index.

The effect of the modulator on a linear polarized light wave is shown in Fig. 9[9]. The plane polarization is declined by 45 degrees to the modulator axis before passing through the modulator. If the optical element is relaxed the light passes through with the polarization unchanged (Fig.9(a)). If the optical element is compressed, the polarization component parallel to the modulator axis travels slightly faster than the vertical component. The horizontal component then "leads" the vertical component after light passes through the modulator (Fig.9 (b)). If the optical element is stretched, the horizontal component "lags" behind the vertical component (Fig.9(c)).

The phase difference between the components at any instant of time is called the retardation. The peak retardation is the amplitude of the sinusoidal retardation as a function of time. The retardation (in length units) is given by

$$A(t)=z[n_x(t)-n_y(t)], \tag{5-1}$$

where $z$ is the thickness of the optical element and $n_x(t)$ and $n_y(t)$ are the instantaneous values of refractive index along the $x$- and $y$- axes, respectively.

An important condition occurs when the peak retardation reaches exactly one-fourth of the wavelength of light. When this happens, the PEM acts as a quarter-wave plate for an instant and causes a 90-degree phase shift between two orthogonal polarization components. Fig.9(d) shows this condition at the instant retardation is at its maximum.

The polarization vector traces a right-handed spiral about the optic axis. Such light is called "right circularly polarized." For an entire modulator cycle, Fig.9(e) shows the retardation vs. time and polarization states at several points in time. The polarization oscillates between right and left circular, with linear (and elliptical) polarization states in between.

### 5-2. Treatment of Circularly Polarized Light

The phase difference for the polarized lights along the $x$- and $y$-axes after passing through the PEM of the length of $d$ is

$$\delta=\delta_x-\delta_y=2\pi\frac{d}{\lambda}(n_x-n_y)=2\pi\frac{d}{\lambda}\Delta n=\delta_0\sin\omega_m t. \tag{5-2}$$

The electric vector of the linearly polarized light which incidents at 45 degrees declined against the principal $x$-axis should change to

$$\begin{aligned}E_m&=\left(\frac{E_0}{\sqrt{2}}\right)\left[e_x\cos\omega\left(\frac{n_x}{c}-t\right)+e_y\cos\omega\left(\frac{n_y}{c}-t\right)\right]\\&=E_0\frac{(e_x+e_y)}{\sqrt{2}}\cos\left(\frac{\delta}{2}\right)\cos\omega\left(\frac{nd}{c}-1\right)\quad(\boldsymbol{E}_{\parallel})\\&+E_0\frac{(-e_x+e_y)}{\sqrt{2}}\sin\left(\frac{\delta}{2}\right)\sin\omega\left(\frac{nd}{c}-1\right)\quad(\boldsymbol{E}_{\perp})\end{aligned} \tag{5-3}$$

$$\begin{aligned}&=\frac{E_0}{\sqrt{2}}\left\{\cos\left(\frac{\delta}{2}\right)+\sin\left(\frac{\delta}{2}\right)\right\}\left\{e_R(1+i)\exp i\omega\left(\frac{nd}{c}-t\right)+(\text{c. c})\right\}\quad(\boldsymbol{E}_R)\\&+\frac{E_0}{\sqrt{2}}\left\{\cos\left(\frac{\delta}{2}\right)-\sin\left(\frac{\delta}{2}\right)\right\}\left\{e_L(1-i)\exp i\omega\left(\frac{nd}{c}-t\right)+(\text{c. c})\right\}\quad(\boldsymbol{E}_L).\end{aligned} \tag{5-4}$$

when the light passed through PEM[10]. Here, $\boldsymbol{E}_{\parallel}$ and $\boldsymbol{E}_{\perp}$ is the amplitudes of the electric vector components, parallel and perpendicular to the polarizer, and $\boldsymbol{E}_R$ and $\boldsymbol{E}_L$ are the amplitudes of the right and left polarized lights. The power of the light is proportional to the amplitude. Therefore, we obtain

$$|\boldsymbol{E}_{R(L)}|^2=\frac{|E_0|^2}{2}\left\{\cos\left(\frac{\delta}{2}\right)\pm\sin\left(\frac{\delta}{2}\right)\right\}^2=\frac{|E_0|^2}{2}(1\pm\sin\delta), \tag{5-5}$$

and the strength of light which has passed through passed the PEM is

$$\begin{aligned}I_m&=I_R+I_L\\&=\frac{I_0}{2}\{1+\sin(\delta_0\sin\omega_m t)\}\quad(I_R).\\&=\frac{I_0}{2}\{1-\sin(\delta_0\sin\omega_m t)\}\quad(I_L)\end{aligned} \tag{5-6}$$

The function $\sin(\delta)$ can be expanded with a Fourier series by the Bessel functions as

$$\cos(\delta)=\cos(\delta_0\sin\omega_m t)=J_0(\delta_0)+2\sum_{n=1}J_{2n}(\delta_0)\cos 2n\omega_m t. \tag{5-7}$$

$$\sin(\delta)=\sin(\delta_0\sin\omega_m t)=2\sum_{n=0}J_{2n+1}(\delta_0)\sin(2n+1)\omega_m t. \tag{5-8}$$

By ignoring the high frequency components, we can understand that the linearly polarized lights are modulated by twice the frequency of the driving frequency of the modulator, whereas the circularly polarized lights are modulated by the same frequency of the modulator. Therefore, we can measure the linearly and circularly polarized lights by lock-in amplified by the frequencies of $2\omega_m$ and$\omega_m$.

The intensity of the light, which is focused onto the detector after passing through the chiral sample, will be described as follows,

$$\begin{aligned} I &= \left(\frac{I_0}{2}\right) 10^{-a_R}\{1+2J_1(\delta_0)\sin\omega_m t+\cdots\} \quad (I_R) \\ &+ \left(\frac{I_0}{2}\right) 10^{-a_L}\{1+2J_1(\delta_0)\sin\omega_m t+\cdots\} \quad (I_L) \\ &= \left(\frac{I_0}{2}\right) 10^{-a}\{(10^{(1/2)\Delta a}+10^{-(1/2)\Delta a}) \quad (I_{DC}) \\ &+ (10^{(1/2)\Delta a}-10^{-(1/2)\Delta a})2J_1(\delta_0)\sin\omega_m t\} \quad (I_{AC}) \end{aligned} \quad , \quad 5\text{-}9)$$

where $\Delta a$ is the difference of the absorbance for LCL and RCL, that is

$$\Delta a = a_L - a_R. \quad 5\text{-}10)$$

The ratio of alternating current and direct current of the frequency of $\omega_m$ is

$$\begin{aligned} \frac{I_{AC}}{I_{DC}} &= 2J_1(\delta_0)\frac{(10^{(1/2)\Delta a}-10^{-(1/2)\Delta a})}{(10^{(1/2)\Delta a}+10^{-(1/2)\Delta a})}G(\tilde{\nu}) \\ &= G(\tilde{\nu})2J_1(\delta_0)\tanh(\ln 10\Delta a/2) \\ &\approx G(\tilde{\nu})J_1(\delta_0)\cdot 2.303\Delta a \end{aligned} \quad , \quad 5\text{-}11)$$

where $G(\tilde{\nu})$ includes the gain of electric circuit, and is a constant intrinsic to the instrument.

## 6. Example of Observed VCD Spectra

The ordinary infrared absorption spectrum and VCD spectrum of $\beta$-pinene have been measured by using a Fourier transform spectrometer, Model Chiral*ir* constructed by Bomem Inc. The measurement conditions are the followings; spectral region: 2000 to 800 $cm^{-1}$, resolution: 4 $cm^{-1}$. The optical path length of liquid cell was adjusted between 15 to 75 $\mu$m so that the absorbance of infrared band to be around 0.4, which is of practical importance to obtain a good VCD signal. We used a liquid nitrogen cooled MCT detector. The accumulation time

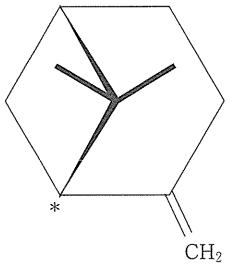


Fig. 10 Molecular structure of (*S*)-$\beta$-pinene
The symbol * denotes the chiral center.

for VCD measurement was 8 hours (50 scans/min).

Raman spectrum was also measured by using a laser Raman spectrometer, Dilor XY. The excitation wavelength was set to 514.5 nm of Ar ion laser.

The *ab initio* theoretical calculations were carried out by using a program package, Gaussian 98[11]. A few combinations of the wavefunctions and basis sets were examined. We chose Hartree-Fock wavefunction or a method depending on the density functional theory (DFT), particularly the B3LYP method. Also examined were a medium size basis set, 4-31G, and a rather large basis set up to 6-31 +G**. First, molecular geometry was optimized and then normal vibration and its IR, Raman, and VCD strength were calculated.

Fig.10 shows the molecular structure of (*S*)-*β*-pinene. Figures 11 to 13 show the parts of the observed spectra of IR, Raman, and VCD. In each figure, the observed spectrum is compared with calculated spectra by the *ab initio* method. The top trace is the observed spectrum, and the next two traces ((a) and (b))

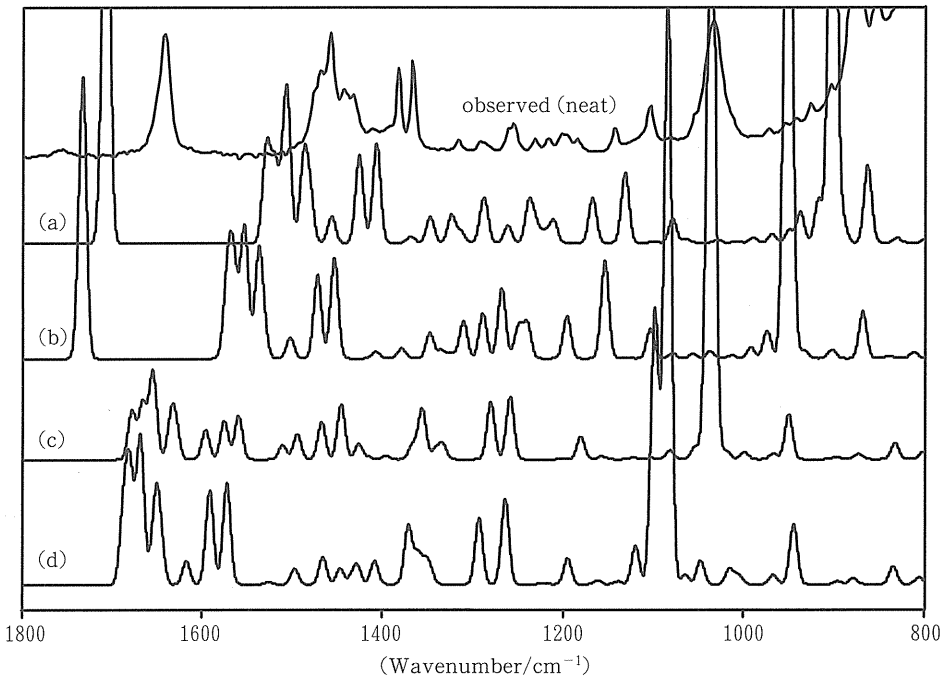


Fig.11 Comparison of observed and calculated IR spectra of(*S*)-*β*-pinene
Top trace is the observed IR spectrum in neat.
(a) Calculated spectrum by B3LYP/6-31+G**,
(b) Calculated spectrum by B3LYP/4-31G,
(c) Calculated spectrum by HF/6-31G*,
(d) Calculated spectrum by HF/4-31G.

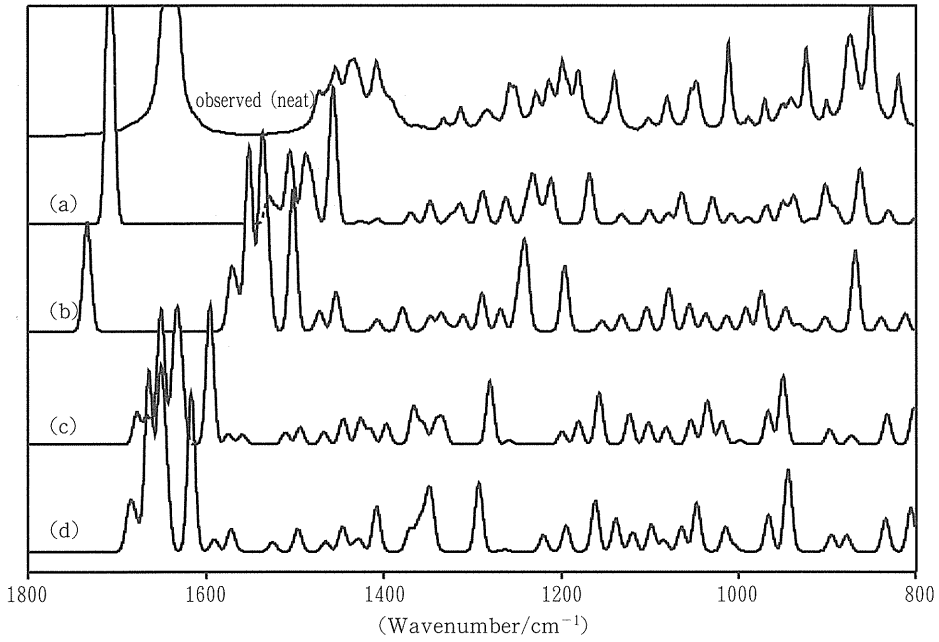


Fig. 12 Comparison of observed and calculated Raman spectra of (*S*)-*β*-pinene
Top trace is the observed Raman spectrum in neat.
(a) Calculated spectrum by B3LYP/6-31+G**,
(b) Calculated spectrum by B3LYP/4-31G,
(c) Calculated spectrum by HF/6-31G*,
(d) Calculated spectrum by HF/4-31G.

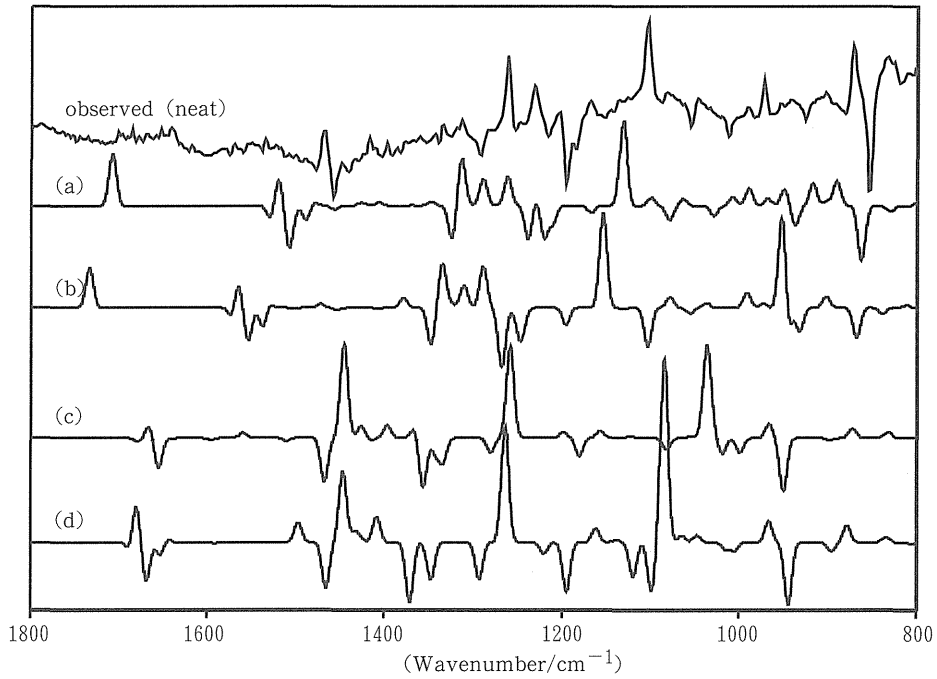


Fig.13 Comparison of observed and calculated VCD spectra of (*S*)-*β*-pinene
Top trace is the observed VCD spectrum in neat.
(a) Calculated spectrum by B3LYP/6-31+G**,
(b) Calculated spectrum by B3LYP/4-31G,
(c) Calculated spectrum by HF/6-31G*,
(d) Calculated spectrum by HF/4-31G.

are the calculated by DFT method, with 6-31+G** and 4-31G, from upper to lower. The bottom two traces ((c) and (d)) are those calculated by HF method, with 6-31G* and 4-31G, from upper to lower.

HF method overestimates the vibrational frequencies as much as 12% and intensities of IR and Raman bands are not in good satisfaction. On the other hand, the DFT method gives the best fit to the observed spectrum, although the vibrational frequencies are still overestimated by about 3%. The lower quality of HF method for VCD prediction is also evident as shown in Fig.13. We also notice that the polarization function is indispensable to obtain a reasonable VCD spectrum. The role of the diffuse function is not clear for the case such as rather stiff molecule like *β*-pinene.

## 7. Structure of Hydrogen-bonding Molecules in Liquid

The molecular structure of 1-amino-2-propanol (AP) is shown in Fig.14. It has

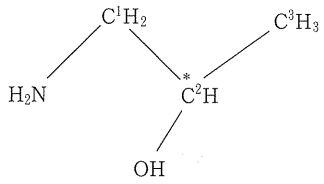


Fig.14 Molecular structure of 1-amino-2-propanol
The symbol * denotes the chiral center.

three carbon atoms as the skeletal backbone. The amino and hydroxyl groups are connected to $C^1$ and $C^2$ carbons, respectively. The $C^2$ atom is the chiral center.

This molecule has four single bonds and three of them, N-$C^1$, $C^1$-$C^2$, and $C^2$-O, give rotational isomerism. Therefore, totally 27 rotational isomers are possible to exist. We first made a geometry optimization for all 27 conformers by HF/4-31G*. The notations for the rotational isomers are defined in Fig.15. The rotational isomers around the N-$C^1$ bond are defined by the dihedral angle made by lone pair and the $C^1$-$C^2$ bond, as g (gauche) and t (trans), and +/− signs indicate the positive (anti-clockwise rotation) and negative (clockwise rotation) dihedral angle. The rotational isomers, T and G around the $C^1$-$C^2$ for the dihedral angle between the amino and hydroxyl groups, and t and g around the $C^2$-O bond for the dihedral angle between the OH and N-$C^1$ bonds are also defined and are shown in Fig.15.

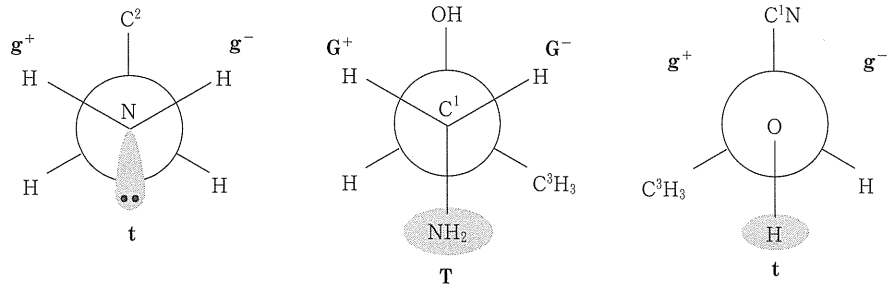


Fig.15 Definitions of rotational isomers of (S)-1-amino-2-propanol

The calculation predicts that the most stable conformer is $g^-G^+g^-$ with population of 74%, and the next population is given to $g^+G^-g^+$ with 14%. These conformers have intramolecular hydrogen bonding between H atom of hydroxyl group and lone pair electrons on amino nitrogen atom as shown in Fig.16. The population of the other conformer is about 1% each. We next applied a method of higher level, B3LYP/6-31++G**, to calculate the geometry and vibrational characters of the stable conformers.

The infrared absorption and VCD spectra were measured by taking the same

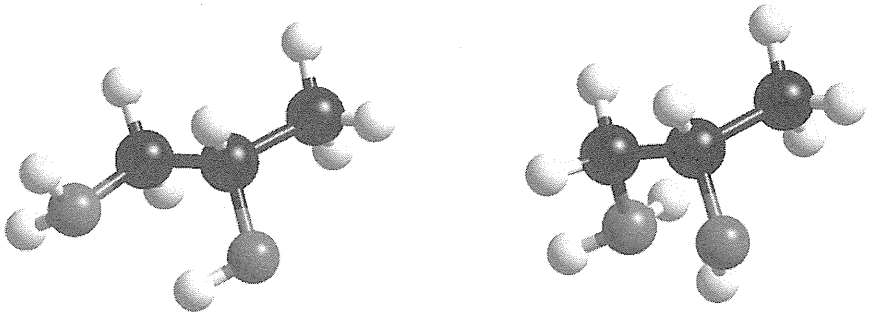

$g^-G^+g^-$ $g^+G^-g^+$

Fig.16 Molecular structures of most stable conformers of (S)-1-amino-2-propanol

care into consideration as described in the previous section. The chiral sample was supplied from Aldrich, Inc. and was used without any purification treatment. The purity of the sample is stated to be about 98% or more. Other than the measurement of neat sample, we investigate the concentration dependence in $CDCl_3$ solvent, from 1.2 to 0.01M. We also measured the spectrum by varying the temperature from 0 to 50℃. The measurement time needed was from 8 to 12 hours to obtain meaningful SN ratio for VCD spectrum.

Top traces of Fig.17 and 18 show the IR and VCD spectra measured for neat sample, and bottom trace shows the predicted spectra for the most stable conformer, $g^-G^+g^-$. The spectral features show rather dramatic changes by lowering the concentration in solution. The broad bands that make continuous background absorption appear as a few distinctive bands. This would reflect the scission of intermolecular hydrogen bonding at lower concentration and the isolation in solvent. In fact, the IR and VCD spectra at low concentration can be fit with *ab initio* spectrum of the most stable form in vacuum. Tam *et al.* concluded[12] that there is no influence of intermolecular hydrogen bonding for VCD spectrum of aminopropanol molecule by judging the results by Qu *et al*[13]. The measurement by Qu *et al.* was done at the concentration of 1 to 2M, which is very dense compared to our experimental condition. There should remain rather strong hydrogen bonding at higher concentration such as 1M.

The VCD bands appearing at 1412 and 1272 $cm^{-1}$ at low concentration have corresponding bands predicted by the *ab initio* calculation for the most stable conformer, $g^-G^+g^-$. The absorption intensities of IR of these bands are weak or medium. Normal coordinate analysis tells that the 1272 $cm^{-1}$ band should be assigned to OH bending, and the 1412 $cm^{-1}$ band has a strong contribution of OH bending mode. The assignment of OH bending has been confirmed by the isotope

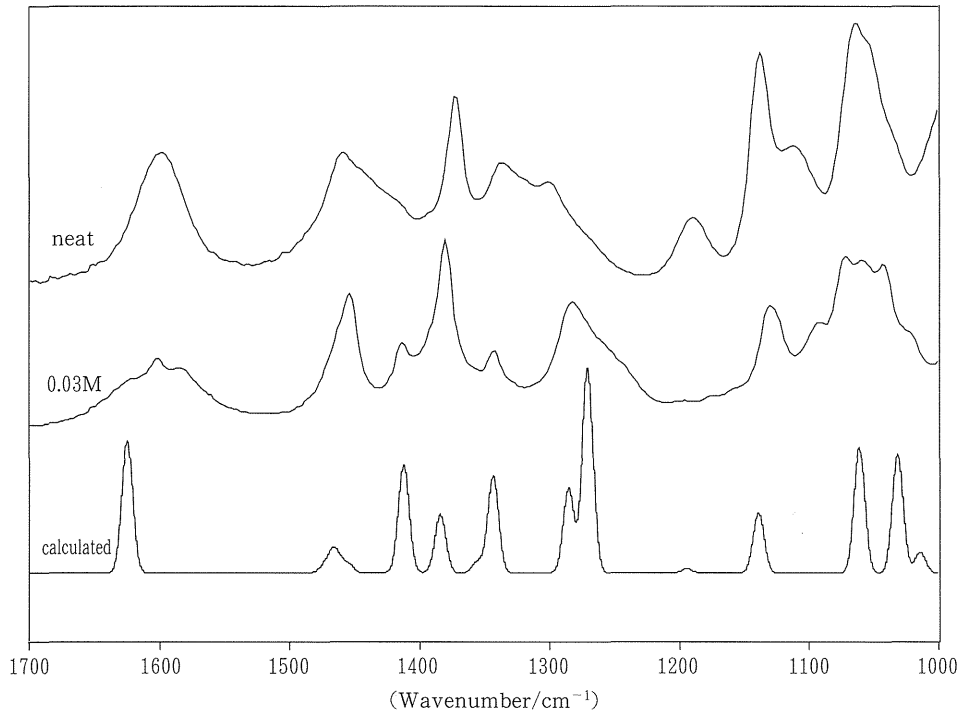


Fig.17 Infrared absorption spectrum of (S)-1-amino-2-propanol

Top trace is the observed IR spectrum in neat. Middle trace is the spectrum of diluted sample (0.3M). Bottom trace is the spectrum of the most stable isomer, $g^{-}G^{+}g^{-}$, calculated by B3LYP/6-31++G** and scaled by 0.98.

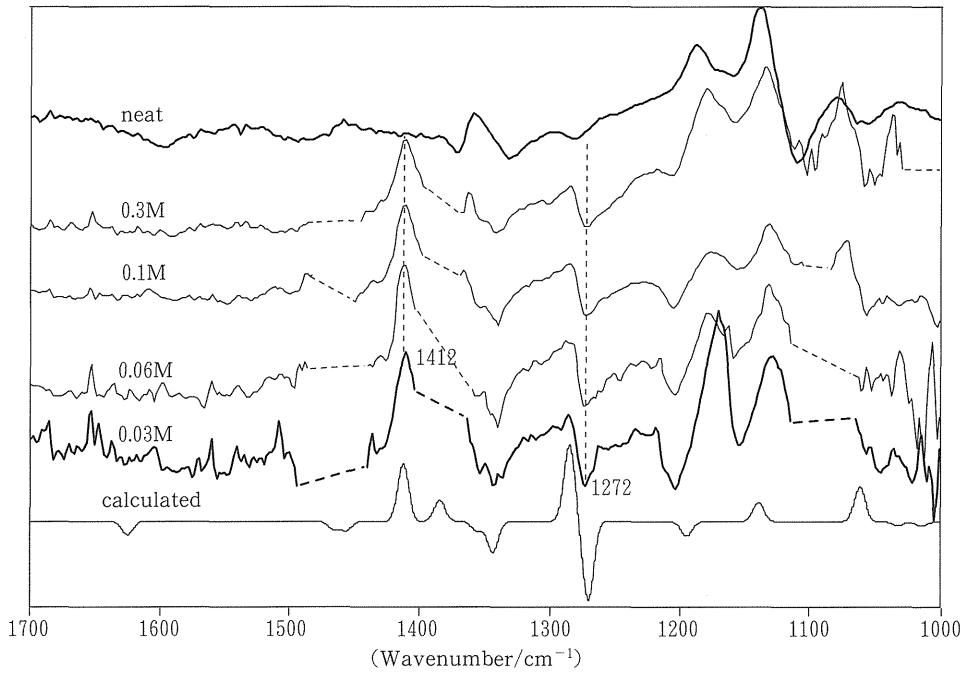


Fig.18 VCD spectrum of (*S*)-1-amino-2-propanol

Top trace is the observed VCD spectrum in neat. Lower traces are the spectra of diluted samples (0.3, 0.1, 0.06, and 0.03M from upper to lower). Bottom trace is the spectrum of the most stable isomer, $g^-G^+g^-$, calculated by B3LYP/6-31++G**. Wavenumbers are scaled by 0.98.

effect. These bands disappear and are shifted to lower wavenumber region by a factor of about $1/\sqrt{2}$ by deuteration of the sample, clearly indicating the assignment that the original bands have the contribution of hydrogen.

Most of the experimental studies on hydrogen bonding system have been focused on OH and NH stretching in 3800 to 3000 $cm^{-1}$ region. We have a valuable piece of information about the dynamics and mechanism of hydrogen bonding from the accumulated data in the stretching region. However, the studies on OH bending are quite limited and there is even a common understanding that OH bending is useless and provides no information on hydrogen bonding[14]. This would be understandable if we know the weak band character and difficulty in identifying the band under the nearby fingerprint bands with stronger intensities.

However, the OH bending band might have a potential value in a study of hydrogen bonding if IR spectrum was combined with VCD spectrum. So far we tried some other molecular systems and obtained nearly the same conclusion.

Further experimental study is needed and we aim to obtain some empirical or theoretical explanation why the VCD band of OH bending appears strongly in hydrogen bonding system and how this information can be correlated to the molecular structure in solution.

## References


1) T. Enomoto, I. Kaneko, K. Kikugawa, and M. Nishijima, in Verandah (in Japanese), Farumashia 35, 895 (1999).
2) T. Shibata, J. Yamamoto, N. Matsumoto, S. Yonekubo, S. Osanai, K. Soai, J. Am. Chem. Soc., 120, 12157 (1998).
3) R. D. Wolstencroft, in "The Search for Extraterrestrial Life: Recent Developments," Ed. by M. D. Papagiannis, International Astronomical Union (1985), p. 171.
4) W. Kuhn, Trans. Faraday Soc., 26, 293 (1930).
5) I. Chabay and G. Holzwarth, Appl. Opt., 14, 454 (1975).
6) E. C. Hsu and G. Holzwarth, J. Chem. Phys., 59, 4678 (1973).
7) G. Holzwarth, E. C. Hsu, H. S. Mosher, T. R. Faulkner, and A. Moscowitz, J. Am. Chem. Soc., 96, 251 (1974).
8) Homepage of Biotools, Inc. http://www.btools.com/bibliography.html.
9) Instruction manual of photoelastic modulators, PEM-90, Hinds instruments, Inc., USA.
10) H. Sugeta, "Measurement method for circular dichroism (in Japanese)" in "Spectroscopy I, Lecture of experimental chemistry Vol. 6" Ed. by Chemical Society of Japan, Maruzen (1991).
11) M. J. Frisch et al. Gaussian 98, Rev. A-7, Gaussian, Inc., Pittsburg, 1998.
12) C. N. Tam, P. Bour, and T. A. Keiderling, J. Am. Chem. Soc., 119, 7061 (1997).
13) X. Qu, M. Citra, N. Ragunathan, T. A. Freedman, L. A. Nafie, Proc. 9th International Conf. on Fourier Transform Spectroscopy, SPIE, 142, 2089 (1993).
14) K. Nakanishi, "Infrared Absorption Spectrum−qualitative analysis and exercise−" Qualitative Analysis (in Japanese) p. 37 Nankodo (1967).


(平成13年11月20日受理)